

Synthesis of Zinc Oxide/Chitosan/Citronella Essential Oil Hybrid Nanoparticles using Sol-Gel Method: Structural and Optical Properties

Budi Astuti^{1*}, Nur 'Ainiyyah Hasni¹, Ari Sulistiyo Rini², Dimas Mohamad Ayubi¹, Agus Yulianto¹, Masturi¹, Teguh Darsono¹, Putut Marwoto¹, Sugianto¹, Suriani Abu Bakar³, Fatiatun⁴,

¹ Physics Study Program, Faculty of Mathematics and Natural Science, University Negeri Semarang, Indonesia

² Physics Department, Faculty of Science, Universitas Riau, Indonesia

³ Physics Department, Faculty of Science, Universiti Pendidikan Sultan Idris Malaysia

⁴ Physics Department, Universitas Sains Al-Quran, Indonesia

Corresponding Author's Email: b_astuti79@mail.unnes.ac.id

Article Info

Article info:

Received: 21-10-2024

Revised: 20-04-2025

Accepted: 07-05-2025

Keywords:

ZnO nanoparticle;
Chitosan; Citronella
essential oil; sol-gel
method; structural
properties; optical
properties

How To Cite:

B. Astuti, N. A. Hasni, A. S. Rini, D. M. Ayubi, A. Yulianto, Masturi, T. Darsono, P. Marwoto, Sugianto, S. A. Bakar, and Fatiatun, "Synthesis of Zinc Oxide/Chitosan/Citronella Essential Oil Hybrid Nanoparticle using Sol-Gel Method: Structural and Optical Properties", *Indonesian Physical Review*, vol. 8, no. 2, p 463-480, 2025.

DOI:

<https://doi.org/10.29303/ipr.v8i2.419>

Abstract

Due to their properties, ZnO nanoparticles have recently been used as an additive material in active food packaging. ZnO has a wide band gap of about 3.37 eV, making it effectively used under UV light. However, ZnO nanoparticles are not effectively used under visible light. This study successfully synthesized ZnO-Chitosan-Citronella Essential Oil hybrid nanoparticles using sol-gel methods. Adding chitosan and citronella essential oil will affect nanoparticles' structural and optical properties. The structural, morphological, and optical properties of characterized hybrid nanoparticles were studied using X-ray diffraction (XRD) and FTIR, scanning electron microscope (SEM), energy dispersive X-ray (EDX), and UV-Vis spectroscopy. From XRD, it was obtained that the ZnO nanoparticles produced have a hexagonal wurtzite crystal structure with angles of $2\theta = 31.76^\circ, 34.48^\circ, 36.30^\circ$ which are crystal planes with orientations (100), (002), and (101), as well as several other peaks for planes (102), (110), (103), (200) and (112) with a crystallinity index value of 86.5390%, and crystallite size of 8.87nm and 7.5335 nm. From FTIR Characterization, Zn=O functional groups were also obtained at wave numbers 657 and 475 cm^{-1} . The morphology of ZnO nanoparticles from SEM spectroscopy shows a spherical shape with agglomeration, and the composition of the components Zn, O, and N elements is found, which come from chitosan materials. Furthermore, from the UV-Vis spectroscopy characterization, it was obtained that the absorption occurred in the 380-600 nm region with a band gap energy of 3.25 eV (using the tauc plot method), which was slightly different from the empirical results of 3.30 eV. The results show potential future studies of hybrid nanoparticles, such as additive materials in active food packaging.



Copyright (c) 2025 by Author(s). This work is licensed under a Creative Commons Attribution-ShareAlike 4.0 International License.

Introduction

Synthesis of metal oxide-based nanomaterials has recently attracted much attention [1]. One of them is the synthesis of zinc oxide (ZnO) nanoparticles, which have wide applications because they have a wide energy band gap of about 3.37 eV and a significant binding energy of 60 meV [2,3]. In addition, ZnO nanoparticles have a stable wurtzite structure with lattice spacing of $a = 0.325$ nm and $c = 0.521$ nm [4-6]. This has attracted much research interest due to its unique optical, acoustic, luminescent, electronic, and optoelectronic properties. In addition to these advantages, ZnO nanoparticles have disadvantages such as a small surface area per volume and an energy band gap unsuitable for use with visible light [7]. The material cannot absorb visible light if the gap energy (E_g) is higher than the visible light energy, which is 3.1 eV. The controlled morphology of ZnO nanoparticles can play a role in minimizing these shortcomings. Other material is also needed to help overcome the problem of minimizing the energy band gap. Because of the narrow band gap, electrons can easily move from the valence band to the conduction band [8]. Thus, ZnO materials are expected to show excitation emission with low excitation energy at visible light. Furthermore, this study modified ZnO by adding Chitosan and Citronella Essential Oil to overcome its weaknesses. Chitosan has low solubility, which can only be dissolved in acidic solvents, but chitosan has biodegradable, antioxidant, and antibacterial properties [9,10]. Meanwhile, Citronella Essential Oil is used because it can increase the ability of active food packaging to block UV rays [11] and increase antibacterial activity [12].

ZnO nanoparticles can be synthesized by several methods, such as the green synthesis method [13], chemical wet method [14], hydrothermal method [15], and sol-gel method [16,17]. Each of these methods has advantages and disadvantages in producing ZnO nanoparticles. For example, the green synthesis method has the advantage that the resulting nanoparticles are environmentally friendly [18]. However, the green synthesis method has disadvantages, namely, the purity of the resulting nanoparticles is not good [19]. Furthermore, the hydrothermal method has advantages, namely the relatively good nanoparticle results and the efficiency of materials in the synthesis process. Still, the process requires relatively expensive costs and high energy [20]. The sol-gel method is quite popular with researchers because the fabrication process is relatively easy, the temperature is not too high, and the purity of the resulting nanoparticles is quite good [21,22]. However, the disadvantage is that it is quite challenging to obtain easily dispersed nanoparticles [23]. According to the advantages and disadvantages of each method, the sol-gel method was chosen to obtain nanoparticles with good purity and at a lower temperature.

This study first aims to synthesize hybrid nanoparticles ZnO/Chitosan/Citronella Essential Oil using the sol-gel method. Second, the obtained ZnO nanoparticles' structural, morphological, and optical properties should be analyzed for further application development as an additive material in active food packaging as an anti-bacterial and light-blocking agent.

Experimental Method

Synthesis of ZnO nanoparticles was carried out using the sol-gel method, referring to [24]. The initial step was to make a chitosan solution by dissolving chitosan in 2% acetic acid as much as 100 mL, and zinc acetate dehydrate (ZAD) with a concentration of 0.68 M as much as 30 mL as precursor. Each solution was stirred using a magnetic stirrer for 15 minutes. After chitosan

and zinc acetate dehydrate (ZAD) solutions were made, both solutions were mixed for 15 minutes using a magnetic stirrer hotplate at a speed of 500 rpm at room temperature. After mixing the solution, 2 mL of citronella essential oil and 0.2 g of sodium tripolyphosphate (STTP) were added as stabilizers.

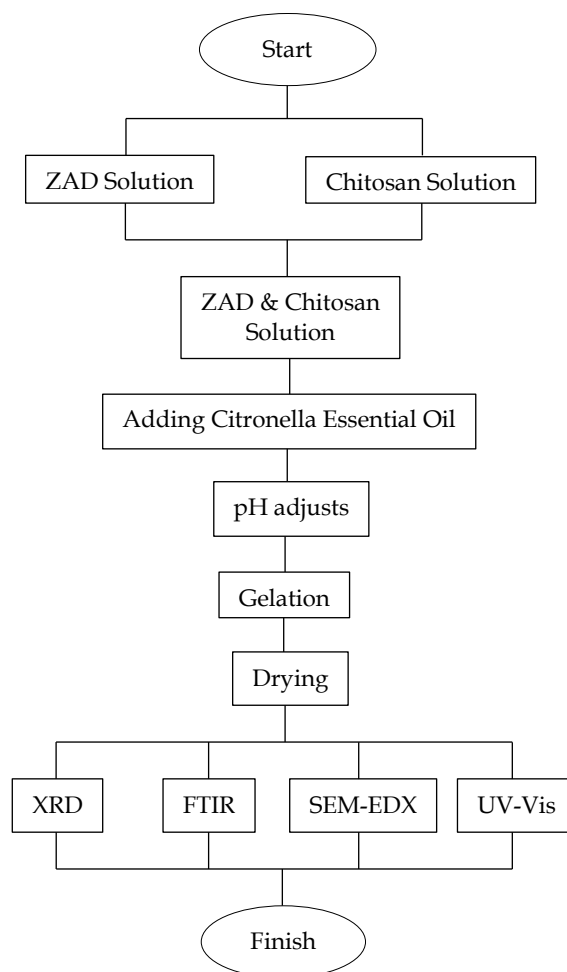


Figure 1. Flow diagram of the experiment process

The solution was stirred for 15 minutes until homogeneous. Furthermore, adjust the pH of the solution to pH = 11 using NaOH (11.25 M) at a temperature of 70 ° C. After obtaining a yellow precipitate, the precipitate was stirred at a temperature of 60 ° C for 4 hours and homogenized using an ultrasonic bath. The precipitate obtained was centrifuged at 6000 rpm for 30 minutes, washed until neutral pH (pH = 7) using pure water. The next step is drying the precipitate at 60°C for 6 hours. Then, the dried precipitate is ground using a mortar, and the final result is nanoparticle powder. The ZnO nanoparticle powder was then characterized using X-ray diffraction (XRD) to determine its structure, and the surface morphology and composition of the ZnO nanoparticle powder were characterized using a scanning electron microscope (SEM) and energy dispersive X-ray (EDX). FTIR characterization was conducted to confirm the

presence of chitosan and citronella essential oil after the synthesis process. The optical properties of ZnO nanoparticle powder's absorption and band gap energy were characterized using UV-Vis spectroscopy.

Result and Discussion

To determine the structural properties of ZnO nanoparticle samples using X-Ray Diffraction (XRD), a Shimadzu 600 with a wavelength of 0.15406nm. XRD characterization was carried out to determine the crystal structure, index, and size of ZnO nanoparticles. In addition, information about the lattice parameters a and c , Zn-O bond lengths, and the volume of unit cells was also analyzed in this paper. The results of the XRD spectrum of ZnO nanoparticle samples with the addition of cithosan and citronella essential oil are shown in Figure 1.

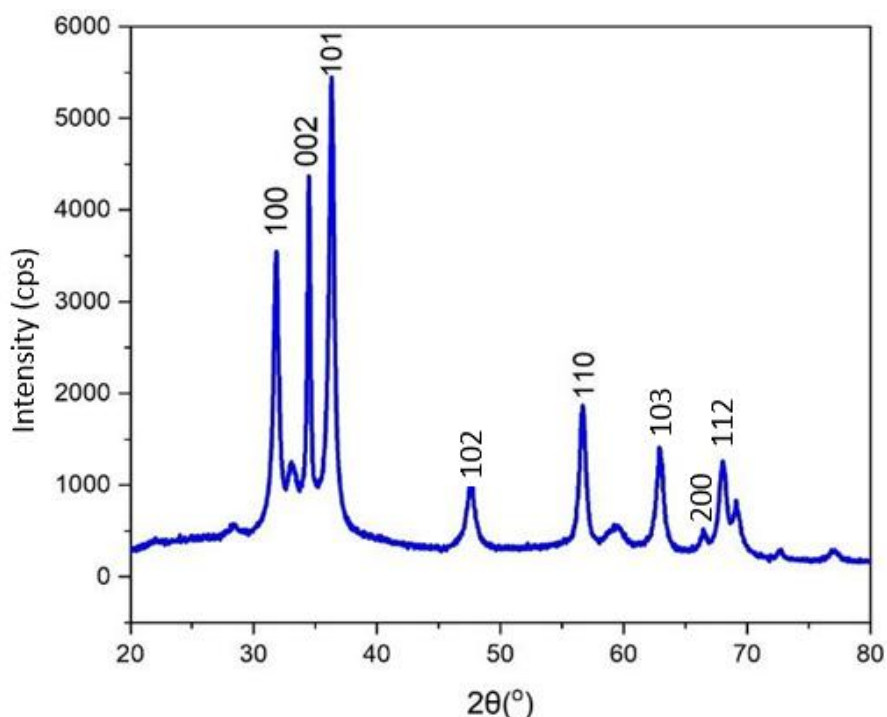


Figure 2. XRD spectrum for ZnO nanoparticles with added cithosan and citronella essential oil.

Based on Figure 2, it can be seen that there are three strong diffraction peaks at 2θ (31.76° , 34.48° , 36.30°) which are crystal planes with orientations (100), (002), and (101), as well as several other peaks for the planes (102), (110), (103), (200) and (112). This pattern refers to pure ZnO and has a hexagonal wurtzite-type structure compared to ICDD cards No. 98-010 [56]. The highest diffraction peak, namely the plane (101), was also reported by Abdullah et al. [28] and Jamdagni et al. [29], which was also shown in this study. In addition, the XRD pattern of ZnO hybrid nanoparticles shows low diffraction peaks at 2θ (22° , 29° , 33° , 59° , 68° , 72° , & 78°), which indicates lower crystallinity from chitosan [57]. This result confirms that chitosan is still present after the synthesis process. Next, the average crystallite size of ZnO NPs was calculated using the Debye-Scherrer equation [30,31] and the Williamson-Hall plot method.

$$D = \frac{0.89\lambda}{\beta \cos\theta} \quad (1)$$

D is the crystallite size, λ is the X-ray source used (0.154 nm), β is the full width at half maximum (FWHM), and θ is the diffraction angle. Detailed analysis of the XRD spectra for crystallite sizes at various reflection angles is shown in Table 1.

Table 1. Analysis of XRD and the assignments of various reflections of ZnO nanoparticle using Debye-Scherrer

Crystal Orientation	Peak Position 2θ (°)	FWHM (°)	Crystallite size D (nm)
100	31.86	1.21	6.75
002	34.44	1.24	6.73
101	36.31	0.82	10.14
102	47.59	0.94	9.20
110	56.67	0.81	11.12
103	62.93	0.82	11.28
112	68.22	1.53	6.27
Average			8.78

Table 2. Analysis of XRD and the assignments of various reflections of ZnO nanoparticle using Williamson-Hall plot method

K	$\lambda(\text{\AA})$	Peak Position	FWHM (°)	X-axis	Y-axis	Crystallite size D (nm)
		2θ	β	$4\sin\theta$	$\beta\cos\theta$	
0.94	1.5406	31.81112	0.48341	1.09621018	0.00811408	7.5335
		34.02385	6.69699	1.170282938	0.111770113	
		34.47459	0.27565	1.185319191	0.004594917	
		36.31574	0.52198	1.246545251	0.008656591	
		47.59693	0.91085	1.614083135	0.014545589	
		56.67005	0.71177	1.89850543	0.01093433	
		62.93554	0.75302	2.088075421	0.011209836	
		68.03589	0.74372	2.23781012	0.010758935	
		69.13362	0.7073	2.269467311	0.010165442	

Based on Table 1 and Table 2, it can be seen that the crystal size of ZnO nanoparticles added with chitosan and citronella essential oil has a nanometer size and this proves that the results of the synthesis of ZnO nanoparticles with chitosan and citronella essential oil using the sol gel method can be said to be nanomaterials because they have fulfilled the characteristics of

nanoparticle size, namely 1-100 nanometers [32]. This result also obtained a lower crystallite size than [36], with an average crystallite size of 20 nm to 41.5 nm, and [56], with an average crystallite size of pure ZnO of 59.725 nm to 75.340 nm, using the same synthesis method. This confirms that adding chitosan and citronella essential oil affects the crystallite size of nanoparticles. Crystallite size affects the anti-bacterial properties of nanoparticles, and a lower crystallite size will increase the anti-bacterial activity [61].

Table 3. Comparison of average crystallite size between this study and the literature

Reference	Nanoparticles (nm)		Average of crystallite size (nm)
This Study	ZnO-Chitosan-Citronella Essential Oil	Debye-Scherrer equation	8.78
		Williamson-Hall plot method	7.5335
[36]	ZnO-Tapioca		20-41.5
[56]	ZnO		59.725-75.340

Another structural property determined from the XRD data is the crystallization index of the ZnO nanoparticle sample. The crystallization index, or crystallinity index, is the percentage of crystallinity of a material [33]. The higher the crystallinity index value of the material or sample, the better the crystal properties. The crystallinity index (Index Crystallinity, CI) is calculated using the equation below, and the detailed calculation results are shown in Table 3. Based on Table 3, it can be seen that the CI value is 86.5390% or around 86.54%. This means that the amount of crystallization in the synthesis process using the sol-gel method is 86.54%. Thus, it can be said that the crystal quality of the ZnO nanoparticle sample is good. This is also confirmed by the sharpness of the diffraction peaks, which are narrow and sharp, indicating that the crystal quality of the resulting ZnO nanoparticles is good, which is also supported by the crystal size value, which is characteristic of the nanomaterial.

$$CI\% = \frac{\text{Total crystallite area}}{\text{Total area}} \times 100\% \quad (2)$$

Table 4. Index crystallinity value

Crystallite Area	Total Crystallite Area	Total Area
3872.61938		
849.29578		
1976.86126		
	17422.74126	20132.79738
4025.87107		
4169.31005		
959.23849		
1569.54523		
Crystallite Index (%)	86.5390	

Furthermore, the lattice parameters a and c can be obtained from the XRD data, which are calculated using the following formula [30, 34].

$$a = \frac{\lambda}{\sqrt{3} \sin \theta_{(100)}} \quad (3)$$

and

$$c = \frac{\lambda}{\sin \theta_{(002)}} \quad (4)$$

For the dislocation density (δ), which indicates crystal defects, and the unit cell volume (V) are calculated using the following equations [31, 35].

$$\delta = \frac{1}{D^2} \quad (5)$$

and

$$V = \frac{\sqrt{3}}{2} a^2 c \quad (6)$$

The bond distance that determines the cation-anion length between Zn and O ions was also studied using the equation [5,34].

$$L = \left(\frac{a^2}{3} + c^2 \left(\frac{1-2u}{2} \right)^2 \right)^{0.5} \quad (7)$$

where u is the position parameter, which is an internal parameter of the ZnO wurtzite phase, which determines the length between Zn and O, where u is the ratio between parameters a and c following the equation [34]

$$u = \frac{1}{4} + \frac{1}{3} \left(\frac{a}{c} \right)^2 \quad (8)$$

The results of the analysis of the calculation of lattice parameters, dislocation density, unit cell volume, and the bond distance are shown in Table 5.

Table 5. Values of lattice parameters, dislocation density, unit cell volume, and the bond distance

Orientation plan (hkl)	$2\theta(^{\circ})$	Lattice (Å)	Parameter	δ ($\times 10^{15} \text{ m}^{-2}$)	$V(\text{\AA})^3$	L (Å)
		$a=b$	c			
(100)	31.86	3.2403		21.95	47.2990	2.0707
(002)	34.44		5.2019	22.08		
(101)	36.31			9.73		

Table 5 shows that the lattice parameters a and c of ZnO nanoparticles added with chitosan and citronella essential oil have values of 3.2403 and 5.2019 Å. The lattice parameter values are the same as the study [36] for ZnO nanoparticles synthesized by an eco-friendly tapioca-assisted route. Thus, the difference in the synthesis method used to produce ZnO nanoparticles does not affect the lattice parameter values a and c , provided that the crystallinity of the ZnO material is formed. Furthermore, it is also shown that the value of the dislocation density for each crystal plane is different. As we know, dislocation is a defect that occurs in a crystal that causes irregularities in the arrangement of atoms in the crystal structure [37]. The presence of dislocations in a crystal can be detrimental or beneficial depending on the application. This is because the presence of dislocations greatly affects the material's properties. The periodic crystal structure will affect the density of the crystal itself. The regularity of the atomic pattern in a crystal will be disturbed by the presence of crystallographic defects, so the movement of dislocations will be hampered by other dislocations appearing in the sample during the synthesis process. As a result, the larger dislocation density value causes the sample to have higher hardness. Thus, it can be said that the ZnO nanoparticle sample with preferred orientation (002) in the hexagonal wurtzite structure has higher hardness properties compared to the crystal orientations (100) and (101). Furthermore, Table 4 shows that the unit cell volume of ZnO nanoparticles with chitosan and citronella essential oil shows a value of 47.2990 (Å)³. As is known, the unit cell volume of a crystal is the smallest volume that undergoes repetition with full crystal structure symmetry.

Figure 3 shows the Fourier-Transform Infrared (FTIR) spectrum comparison of ZnO-Chitosan-Citronella Essential Oil, pure chitosan [58], and pure citronella essential oil [59]. ZnO nanoparticles with chitosan and citronella essential oil have a spectrum in the range of 400-4000 cm⁻¹, which strengthens the qualitative data from the XRD results. The spectrum confirms the formation of ZnO with a vibration band (475 cm⁻¹), which is a stretching band of Zn-O [30, 38]. Figure 3 also shows a vibration peak at 3430 cm⁻¹, an O-H group stretching vibration that is possible as an oscillation of water molecules [39, 40, 41]. The transmission peak was also observed in the 1560 cm⁻¹ region, which is a symmetrical stretching of C=O [42]. Furthermore, the maximum and sharpest absorption peak intensity was observed in the 1412 cm⁻¹ region, which is a vibration band of the C-O-H and C-H bending groups [37]. The peak observed at 1051 cm⁻¹ is associated with the functional group of free amino (-NH₂) [58]. The band observed at 833 cm⁻¹ is the deformation vibration of water molecules [44]. However, in other references, absorption at wave number 831 cm⁻¹ is the vibration and bending modes of CO₃²⁻ [45, 46]. The bands observed at 657 and 475 cm⁻¹ are vibrations caused by the presence of metal oxides, which are Zn-O stretching vibration [47, 48]

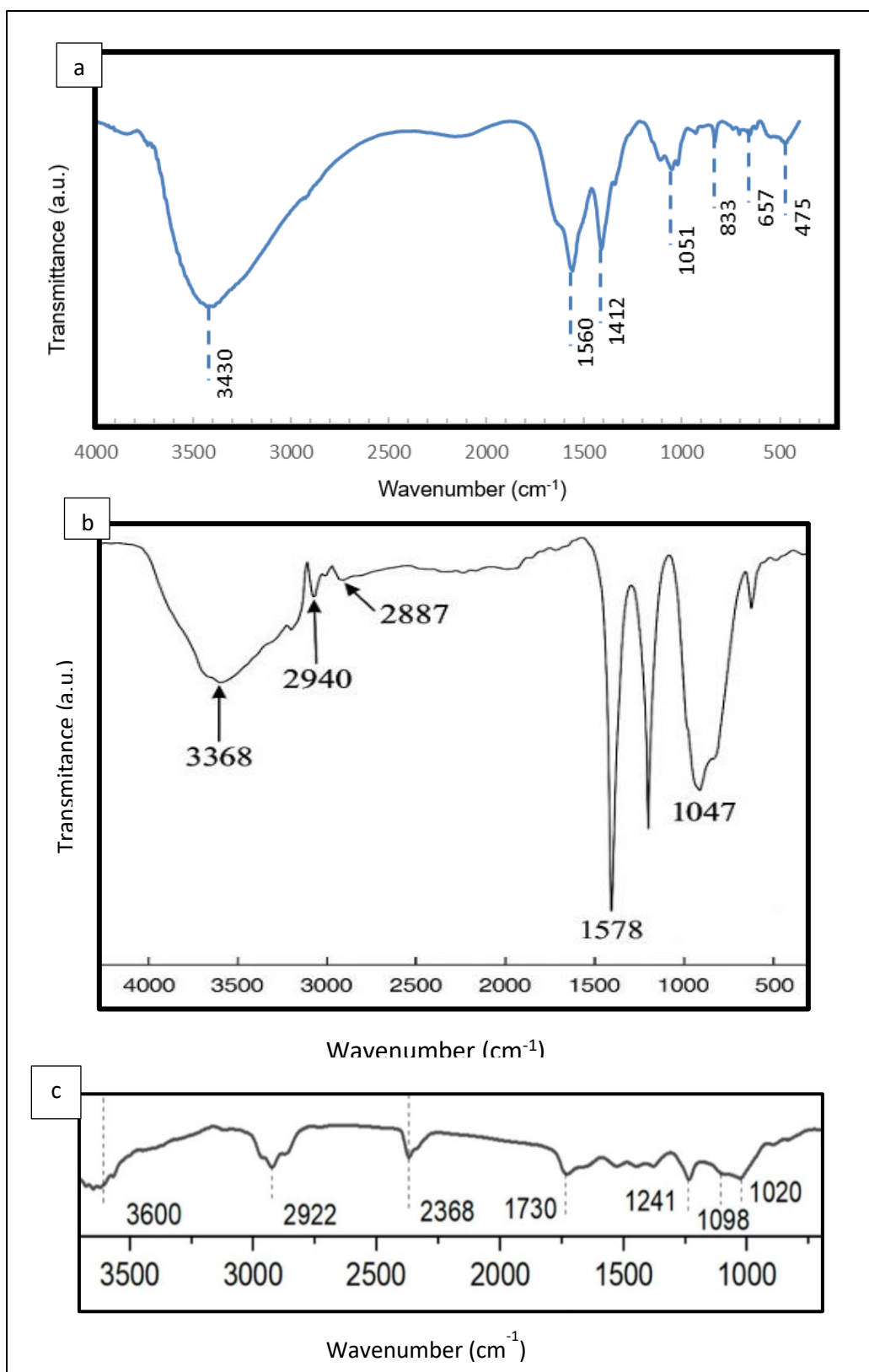


Figure 3. (a) FTIR spectrum of ZnO Nanoparticles (b) FTIR spectrum of pure chitosan [58] (c) FTIR spectrum of pure citronella essential oil [59].

Surface Morphology Characterization

Scanning Electron Microscope (SEM) Phenom Pro-X was used to determine the surface morphology of ZnO nanoparticles added with chitosan and citronella essential oil. The morphology in the form of size and structure of the particles was tested to determine whether the resulting particles met the requirements as nanomaterials. The test results using a voltage of 15 KV with a magnification of 7.5K and 30K are shown in Figure 4.

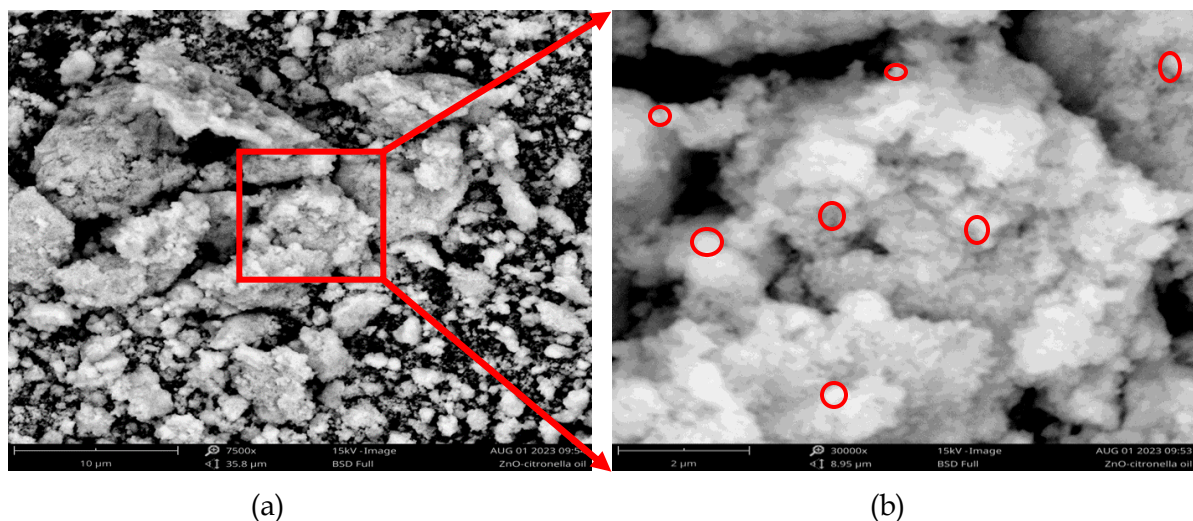


Figure 4. SEM image-surface morphology with magnification (a) 7.5K and (b) 30K

Table 6. Average particle size using ImageJ

No	Particle Size (nm)	Average (nm)
1	31.03	46.532
2	30.00	
3	33.41	
4	44.32	
5	31.02	
6	70.60	
7	69.29	
8	57.90	
9	34.98	
10	62.77	

Based on Figure 4, it can be seen that the morphology of ZnO nanoparticles shows a spherical shape [49]. From the SEM image, it can also be observed that agglomeration occurs in ZnO nanoparticles, so that the nanoparticles still do not form a perfect sphere. Agglomeration can occur because there is a weak force between particles caused by the weak force of the particle core [50]; this effect could be influenced by an unstable pH value [60]. Furthermore, using ImageJ software, from SEM characterization, particle size measurements were carried out from

10 points, and it was obtained that the diameter of ZnO nanoparticles was in the range of 30.0 to 70.6 nm, with an average diameter of 46.532 nm, as shown in Table 6. This shows that ZnO nanoparticles added with chitosan and citronella essential oil have been included in the nanomaterial category [51]. These results also confirm the results of the previous XRD analysis. Although there are differences in the measurement results of the crystal size from XRD and SEM measurements, this is because in XRD, there is a direct interaction between X-rays and the constituent atoms, while in SEM, ZnO nanoparticle powder experiences agglomeration, so that the measured particle size is a combination of several ZnO particles themselves.

Next, the composition of ZnO nanoparticles was tested using EDX (Energy Dispersive X-Ray) Phenom Pro-X. The result of EDX characterization is shown in Figure 5, and the composition of ZnO nanoparticles can be seen in Table 6.

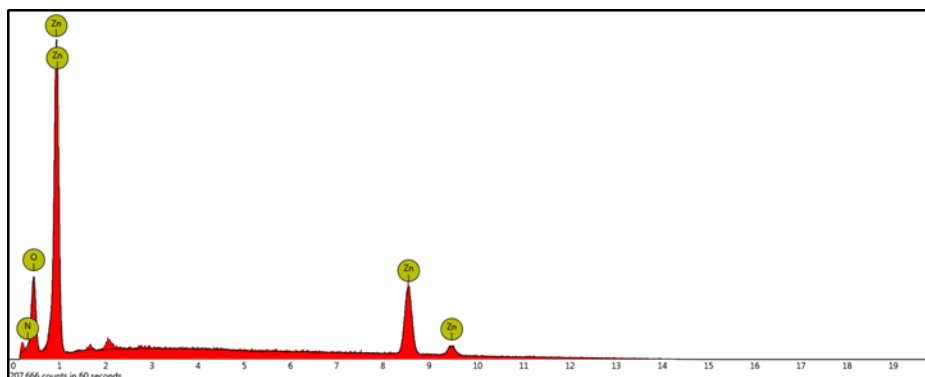


Figure 5. Composition of ZnO nanoparticles with chitosan and citronella essential oil

Table 7. Composition of ZnO nanoparticles with chitosan and citronella essential oil

Element Symbol	Atomic Conc. (%)	Weight Conc. (%)
Zn	50.15	80.87
O	38.71	15.28
N	11.14	3.85

Based on Table 7, it can be seen that the composition of ZnO nanoparticles synthesized by the sol-gel method is well-formed, with no contaminant elements. The detected nitrogen element also indicates that chitosan has perfectly blended with ZnO nanoparticles, which are dopants to reduce the large band gap energy and improve the performance of ZnO nanoparticles so that they can become safe additives supported by the Chitosan material.

Optical Properties of ZnO Nanoparticles

The optical properties of the prepared ZnO nanoparticle samples were studied using UV-Vis spectroscopy characterization. It can be seen in Figure 6 that there is intensive absorption in the UV-visible-NIR region, with low to medium energy absorption between about 420–600 nm. A sharp increase in absorbance located around 380 nm was also observed, related to the intrinsic band gap absorption of ZnO, and attributed to the promotion of electrons in the semiconductor from the valence band (VB) to the conduction band (CB) [36, 37, 52]. The high absorption increase is assumed to be due to the smaller size of ZnO nanoparticles Tadj et al.

[53]. This follows the results of XRD characterization, where the ZnO nanoparticle sample has a small crystallite size of about 8.78 nm, resulting in high UV light absorption.

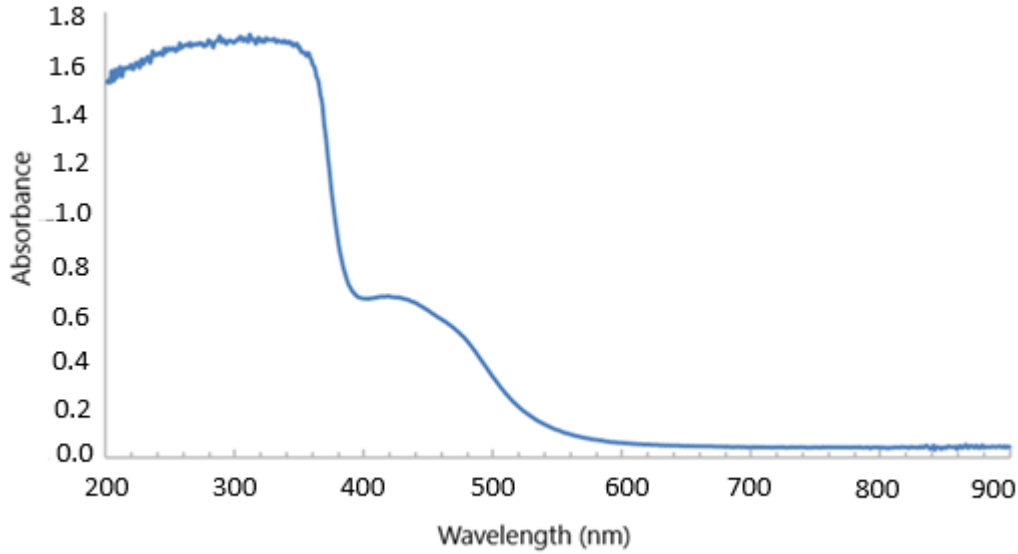


Figure 6. Uv-Vis Spectrum of ZnO nanoparticles

Furthermore, from the UV-Vis spectroscopy characterization, the optical band gap of the semiconductor or the energy band gap can be determined using the Tauc plot equation [47,54] as shown in Figure 6. This methodology uses direct band gap (E_g) data processing, as recommended for ZnO [37, 52].

$$\alpha h\nu = A(h\nu - E_g)^{0.5} \quad (9)$$

where A is a constant, $h\nu$ is the photon energy, E_g is the allowed energy gap, and $n = 1/2$ for allowed direct transition. The Tauc's region tells the structural and thermal disorder present in the nanoparticle [47]. The synthesized ZnO nanoparticle sample's band gap (E_g) value was obtained at 3.25 eV. The E_g value is lower than the E_g value for ZnO material in bulk size. In addition to using the Tauc plot method, the E_g value is also empirically determined using the effective mass model [37,55].

$$E_g^{Nano} = E_g^{Bulk} + \frac{h^2}{8\epsilon r^2} \left[\frac{1}{m_e} + \frac{1}{m_h} \right] - \frac{1.8e^2}{4\pi\epsilon\epsilon_0 r} \quad (10)$$

Where E_g^{Bulk} is 3.37 eV, h is planck constant 6.626×10^{-34} Js, e is elementary charge of the electron, 1.602×10^{-19} C, m_e is effective electron mass, 2.1864×10^{-31} Kg, m_h is effective hole mass, 4.0995×10^{-31} Kg, ϵ is relative permittivity, 8.66, ϵ_0 is vacuum permittivity, 8.864×10^{-12} F/m, and r is the radius calculated from the crystallite size obtained by XRD. Based on the calculation using the equation, it was obtained as much as 3.30 eV. Furthermore, the calculation was carried out. Although there is a difference in the E_g value obtained from the Tauc plot method and equation (10), the E_g (nano) results strengthen the E_g value obtained from the Tauc plot method, because both calculation methods hatendo reduce E_g when the crystallite size becomes large [53].

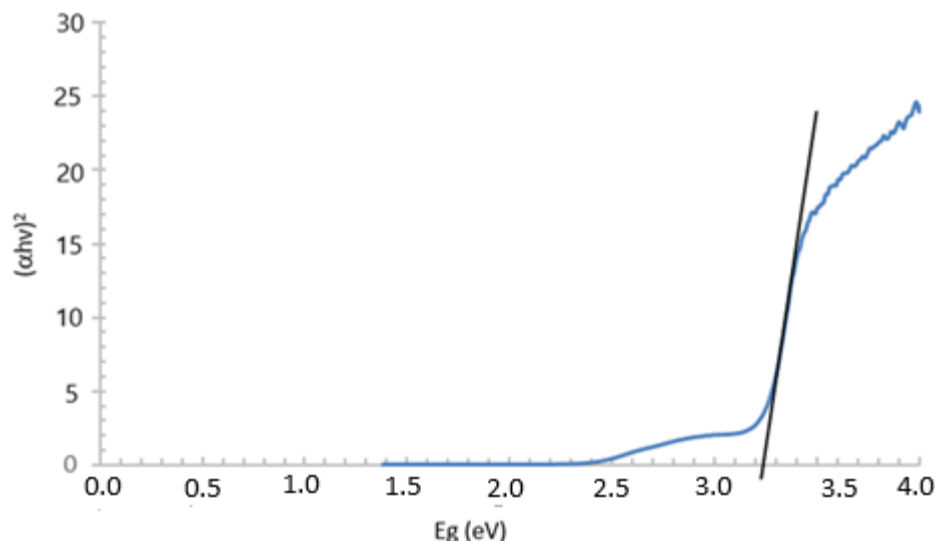


Figure 7: Tauc plot method of the ZnO nanoparticle sample

Conclusion

ZnO-Chitosan-Citronella Essential Oil Hybrid Nanoparticles have been successfully prepared. EDX and FTIR confirm the presence of ZnO, chitosan, and citronella essential oil. The morphology of ZnO nanoparticles from SEM spectroscopy shows a spherical shape with agglomeration, and the composition of the components does not contain contaminants, because only Zn, O, and N elements are found in chitosan materials. The agglomeration could be affected by an unstable pH value. Based on the results of XRD characterization, it was obtained that ZnO nanoparticle powder has a hexagonal wurtzite crystal structure with angles of $2\theta = 31.76^\circ, 34.48^\circ, 36.30^\circ$ which are crystal planes with orientations (100), (002), and (101), as well as several other peaks for the planes (102), (110), (103), (200) and (112) with a crystallinity index value of 86.5390%. Hybrid nanoparticles show good results in crystallite size compared to pure ZnO nanoparticles from previous studies. Crystallite size of hybrid nanoparticle obtained by using Debye Scherrer equation and Williamson-Hall plot method obtained as much as 8.87 nm and 7.5335 nm. In addition, calculations were also carried out on the lattice parameters a , and c of 3.2403 Å and 5.2019 Å, dislocation density of $21.95 \times 10^{15} \text{ m}^{-2}$, the volume of the ZnO crystal unit cell of 47.2990 (Å)³, and the Zn-O bond distance of 2.0707 Å. Furthermore, from the UV-Vis spectroscopy characterization, it was obtained that the absorption occurred in the 380-600 nm region with a band gap energy of 3.25 eV (using the tauc plot method), which was slightly different from the empirical results of 3.30 eV. From this result, it can be concluded that adding chitosan and citronella essential oil could help minimize the crystallite size and energy gap of the hybrid nanoparticles. The crystallite size obtained in this study shows a significant result. However, the energy gap result does not significantly decrease. For future studies, an antibacterial test for the sample might be conducted to confirm the antibacterial activity of hybrid nanoparticles. Chitosan and citronella essential oil variations might be conducted to decrease the energy gap so that the hybrid nanoparticles could effectively work in visible light.

Acknowledgment

The author would like to thank the Faculty of Mathematics and Natural Sciences, Semarang State University, through DPA funding in 2024. 180.28/UN37/PPK.04/2024. In addition, the author would also like to thank Nathalia Erna S., Radhotul Muttaqin, and Agus Nu'man for their contributions to the characterization process carried out and for facilitating this research.

References

- [1] D.M. Tajashwini, H.V. Harini, H.P. Nagaswarupa, R. Naik, V.V. Deshmukh, and N. Basavaraju, "An in-depth exploration of eco-friendly synthesis method for metal oxide nanoparticle and their role in photocatalysis for industrial dye degradation, chemical physics impact, vol. 7, pp. 100355, 2023.
- [2] C. Abed, S. Fernandes, S. Aouida, H. Elhouichet, F. Priego, Y. Castro, M.M. Gomes-Mancebo, and G. Munuera, "Processing and study of optical and electrical properties of (Mg, Al) co doped ZnO thin films prepared by RF magnetron sputtering for photovoltaic application". *Materials*. Vol. 13, no. 9, pp. 1-12, 2020.
- [3] B. Astuti, P. Marwoto, A. Zhafirah, N. Hamid, D. Aryanto, S. Sugianto, S. Sulhadi, N. M. D. Putra, and F. Fianti, "Structure, morphology, and optical properties of ZnO:Mg thin film prepared by sol-gel spin coating method", *Jurnal Ilmiah Pendidikan Fisika Al-BiRuNi*, Vol. 10. No. 2. Pp. 75-84, 2021.
- [4] M. Bakry, W. Ismail, M. Abdelfatah, and A. El-Shaer, "Low-cost fabrication methods of ZnO nanorods and their physical and photoelectrochemical properties for optoelectronic applications", *Scientific Reports Nature Portfolio*, Vol. 14, pp. 23788, 2024.
- [5] B. Astuti, A. Zhafirah, V. A. Carieta, N Hamid, P Marwoto, S. Sugianto, U. Nurbaiti, F. D. Ratnasari, N. M. D. Putra, and D. Aryanto, "X-ray diffraction studies of ZnO:Cu thin films prepared using sol-gel method", *Journal of Physics: Conference Series*, Vol. 1567, pp. 022004, 2020.
- [6] P. Laokul, N. Kanjana, R. Ratchatanee, S. Ruangjan, N. Kotsarn, A. Chingsungnoen, and P. Poolcharuansin, "Preparation of AgBr decorated ZnO/ZnS nanocomposite for photocatalytic and antibacterial applications", *Materials Chemistry and Physics*, Vol. 295. Pp. 127112, 2023.
- [7] J. Gaur, S. Kumar, M. Pal, H. Kaur, K.M. Batoo, J.O. Momoh, and Supreet, "Current trends: Zinc oxide nanoparticles preparation via chemical and green method for the photocatalytic degradation of various organic dyes", *Hybrid Advances*, Vol. 5, pp.100128, 2024.
- [8] S. Lee, K.H. Jin, H. Jung, K. Fukutani, J. Lee, C. Kwon, J. S. Kim, J. Kim, and H. W. Yeom, "Surface Doping and Dual Nature of the Band Gap in Excitonic Insulator Ta₂NiSe₅", : *ACS Nano*, Vol. 18, pp. 24784–24791, 2024.
- [9] W. Wang, C. Xue, and X. Mao, "Chitosan: Structural modification, biological activity and application, Vol. 164, pp. 4532-4546, 2020.

- [10] I. Aranaz, A.R. Alcántara, M.C. Civera, C. Arias, B. Elorza, H.A. Caballero, and N. Acosta, "Chitosan: An Overview of Its Properties and Applications", *Polymers*, Vol. 13, No. 19, pp. 3256, 2021.
- [11] E. Zabihi, A. Babaei, D. Shahrampour, Z. Arab-Bafrani, K.S. Mirshahidi, and H.J. Majidi, "Facile and Rapid in-situ Synthesis of Chitosan- ZnO Nano-Hybrids Applicable in Medical Purposes; a Novel Combination of Biomineralization, Ultrasound and Bio-Safe Morphology-Conducting Agent", *International Journal of Biological Macromolecules*, Vol. 131, pp. 107-116, 2019.
- [12] L. Motelica, D. Fica, O. Oprea, A. Fica, R.D. Trusca, E. Andronescu, and A.M. Holban, "Biodegradable Alginate Films with ZnO Nanoparticles and Citronella Essential Oil – A Novel Antimicrobial Structure. " Vol. 13 No. 7, pp. 1020, 2021.
- [13] T.A.J. De Souza, L.R.R. Souza, and L.P. Franchi, "Silver Nanoparticles: An Integrated View of Green Synthesis Methods, Transformation in The Environment, and Toxicity". *Ecotoxicology and environmental safety*, Vol. 171, pp. 691-700, 2019.
- [14] M.M. Baig, M.A. Yousuf, P.O. Agboola, M.A. Khan, I. Shakir, and M.F. Warsi, "Optimization of Different Wet Chemical Routes and Phase Evolution Studies of MnFe₂O₄ Nanoparticles Vol. 45, No. 10, pp. 12682-12690, 2019.
- [15] Basnet, P., & Chatterjee, S. (2020). Structure-Directing Property and Growth Mechanism Induced by Capping Agents in Nanostructured ZnO During Hydrothermal Synthesis – A Systematic Review. *Nano-Structures & Nano-Objects*, 22, 100426.
- [16] R.L. Manjunatha, D. Naik, and K.V. Usharani, "Nanotechnology Application in Agriculture: A review", *Journal of Pharmacognosy and Phytochemistry*, Vol. 8, No. 3, pp. 1073-1083, 2019.
- [17] M. Parashar, V.K. Shukla, and R. Singh, "Metal Oxides Nanoparticles Via Sol-Gel Method: a Review on Synthesis, Characterization and Applications. *Journal of Materials Science: Materials in Electronics*, Vol. 31, pp. 3729-3749, 2020.
- [18] J. Singh, T. Dutta, K.H. Kim, M. Rawat, P. Samddar, and P. Kumar, "Green 'synthesis of metals and their oxide nanoparticles: applications for environmental remediation", *Journal of nanobiotechnology*, Vol. 16 No. 1, pp. 1-24, 2018.
- [19] S. Ying, Z. Guan, P.C. Ofoegbu, P. Clubb, C. Rico, F. He, and J. Hong, "Green Synthesis of Nanoparticles: Current Developments and Limitations", *Environmental Technology & Innovation*, Vol. 26, pp. 102336, 2022.
- [20] Y.X. Gan, A.H. Jayatissa, Z. Yu, X. Chen, and M. Li, "Hydrothermal Synthesis of Nanomaterials", *Journal of Nanomaterials*, Vol. 2020, pp. 1-3, 2020.
- [21] M. D'Arienzo, R. Scotti, B. Di Credico, and M. Redaelli, "Synthesis and Characterization of Morphology-Controlled TiO₂ Nanocrystals: Opportunities and Challenges for Their Application in Photocatalytic Materials", *Studies in Surface Science and Catalysis*, Vol. 177, pp. 477-540, 2017.
- [22] D. Navas, S. Fuentes, A. Castro- Alvarez, and E. Chavez-Angel, "Review on sol-gel synthesis of perovskite and oxide nanomaterials. *Gels*. Vol. 7, No. 4, pp. 275, 2021.

- [23] R. Paul, "Sol-Gel Method: Overcoming the Limitation in Nanoparticle Synthesis, Vol. 11, pp. 008, 2023.
- [24] T. Gasti, S. Dixit, V.D. Hiremani, R.B. Chougale, S.P. Masti, S.K. Vootla, and B.S. Mudigoudra, "Chitosan/Pullulan Based Films Incorporated with Clove Essential Oil Loaded Chitosan-ZnO Hybrid Nanoparticles for Active Food Packaging", *Carbohydrate Polymers*, Vol. 277, pp. 118866, 2022.
- [25] S.C. Chabattula, P.K. Gupta, S.K. Tripathi, R. Gahtori, P.Padhi, S. Mahapatra, B.K. Biswal, S.K. Singh, K. Dua, J. Ruokolainen, Y.K. Mishra, N.K. Jha, D.K. Bishi, and K.K. Kesari, "Anticancer therapeutic efficacy of biogenic Am-ZnO nanoparticles on 2D and 3D tumor models", *Materials Today Chemistry*, Vol. 22, pp. 100618, 2021.
- [26] G. Sathishkumar, C. Rajkuberan, K. Manikandan, S. Prabukumar, J. DanielJohn, S. Sivaramakrishnan, "Facile biosynthesis of antimicrobial zinc oxide (ZnO) nanoflakes using leaf extract of *Couroupita guianensis* Aubl.", *Materials Letters*, Vol. 188, pp. 383-386, 2017.
- [27] A.M Ismail, A.A. Menazea, H.A. Kabary, A.E. El-Sherbiny, and A. Samy, "The Influence of Calcination Temperature on Structural and Antimicrobial Characteristics of Zinc Oxide Nanoparticles Synthesized by Sol-Gel Method", *Journal of Molecular Structure*, Vol. 1196, pp. 332-337, 2019.
- [28] K. A Abdullah, S. Awada, J. Zaraket and C. Salame, "Synthesis of ZnO Nanopowders By Using Sol-Gel and Studying Their Structural and Electrical Properties at Different Temperature", *Energy Procedia*, Vol. 119, pp. 565-570, 2017.
- [29] P. Jamdagni, P. Khatri, and J.S. Rana, "Green synthesis of zinc oxide nanoparticles using flower extract of *Nyctanthes arbor-tristis* and their antifungal activity", *J. King Saud Univ. Sci.* Vol. 30, pp. 168e175, 2018.
- [30] B. Bulcha, J. L. Tesfaye, D. Anatol, R. Shanmugam, L.P. Dwarampudi, N. Nagaprasad, V. L. Nirmal Bhargavi, and R. Krishnaraj, "Synthesis of Zinc Oxide Nanoparticles by Hydrothermal Methods and Spectroscopic Investigation of Ultraviolet Radiation Protective Properties", *Hindawi Journal of Nanomaterials*, Vol. 2021, pp. 8617290, 2021.
- [31] B. Astuti, N. Abidah, E.A. Fatiha, and K.A. Nugraha, "Structure and morphology analysis of annealing post-treatment thin film titanium and copper-doped zinc oxide", *Indonesian Physical Review*, Vol. 6, No. 3, pp. 334-345, 2023.
- [32] I. Khan, K. Saeed, and I. Khan, "Nanoparticles: Properties, Applications and Toxicities", *Arabian Journal of Chemistry*, Vol. 12, No. 7, 908-931, 2019.
- [33] I. Uzun, "Methods of determining the degree of crystallinity of polymers with X-ray diffraction: a review", *Journal of Polymer Research*, Vol.30, pp. 394, 2023.
- [34] S. Mansy, H. Musleh, S. Shaat, J. Asad, and N. Al Dahoudi, "Computational and experimental study of wurtzite phase ZnO nanoparticles", *MaterialsTodayCommunications*, Vol. 35, pp. 105688, 2023.
- [35] M. Kahouli, A. Barhoumi, Anis Bouzid, A. Al-Hajry, and S. Guermazi, "Structural and optical properties of ZnO nanoparticles prepared by direct precipitation method", *Superlattices and Microstructures*, Vol. 85, pp. 7-23, 2015.

- [36] W. L. de Almeida, N. S. Ferreira, F. S. Rodembusch, and V. C. de Sausa, "Study of structural and optical properties of ZnO nanoparticles synthesized by an eco-friendly tapioca-assisted route", *Materials Chemistry and Physics*, Vol. 258, pp. 123926, 2021.
- [37] W. L. de Almeida, L. C. Freisleben, B. C. Brambilla, V. G. Isoppo, F. S. Rodembusch, V. C. de Sousa, "Influence of starch used in the sol-gel synthesis of ZnO nanopowders", *J Nanopart Res*, Vol. 25, pp. 75, 2023.
- [38] M. S. Choi, H. G. Na, G. S. Shim et al., "Simple and scalable synthesis of urchin-like ZnO nanoparticles via a microwave-assisted drying process," *Ceramics International*, vol. 47, no. 10, pp. 14621–14629, 2021.
- [39] K. F. Hasan, H. Wang, S. Mahmud, and C. Genyang, "Coloration of aramid fabric via in-situ biosynthesis of silver nanoparticles with enhanced antibacterial effect," *Inorganic Chemistry Communications*, vol. 119, p. 108115, 2020.
- [40] A. K. Dikshit, P. Banerjee, N. Mukherjee, and P. Chakrabarti, "Theoretical optimization of double dielectric back reflector layer for thin c-Si based advanced solar cells with notable enhancement in MAPD," *Superlattices and Microstructures*, vol. 149, p. 106747, 2021.
- [41] J. A. Delezuk, D. E. Ramírez-Herrera, B. Esteban-Fernández de Ávila, and J. Wang, "Chitosan-based water-propelled micro motors with strong antibacterial activity," *Nanoscale*, vol. 9, no. 6, pp. 2195–2200, 2017.
- [42] N. A. Ibrahim, A. A. Nada, B. M. Eid, M. Al-Moghazy, A. G. Hassabo, and N. Y. Abou-Zeid, "Nano-structured metal oxides: synthesis, characterization and application for multifunctional cotton fabric," *Advances in Natural Sciences: Nanoscience and Nanotechnology*, vol. 9, no. 3, p. 035014, 2018.
- [43] S. M. Costa, D. P. Ferreira, A. Ferreira, F. Vaz, and R. Fangueiro, "Multifunctional flax fibres based on the combined effect of silver and zinc oxide (Ag/ZnO) nanostructures," *Nanomaterials*, vol. 8, no. 12, p. 1069, 2018.
- [44] R. Pandimurugan and S. Thambidurai, "UV protection and antibacterial properties of seaweed capped ZnO nanoparticles coated cotton fabrics," *International Journal of Biological Macromolecules*, vol. 105, Partt 1, pp. 788–795, 2017.
- [45] S. Mohan, M. Vellakkat, A. Aravind, and U. Reka, "Hydrothermal synthesis and characterization of Zinc Oxide nanoparticles of various shapes under different reaction conditions", *NanoExpress*, vol. 1, pp. 030028, 2020.
- [46] H. H.A. Alshamsi, and B.S. Hussein, "Hydrothermal preparation of silver-doped zinc oxide nanoparticles: studies, characterization and photocatalytic activities", *Orient. J. Chem*, vol. 34, pp. 1898, 2018.
- [47] P. Ramesh, K. Saravanan, P. Manogar, J. Johnson, E. Vinoth, and M. Mayakannan, "Green synthesis and characterization of biocompatible zinc oxide nanoparticles and evaluation of its antibacterial potential", *Sensing and Bio-Sensing Research*, vol. 31, pp. 100399, 2021.
- [48] X. Xiao, B. Peng, L. Cai, and X. Zhang, "The highly efficient catalytic properties for thermal decomposition of ammonium perchlorate using mesoporous ZnCo₂O₄ rods synthesized by the oxalate co-precipitation method", *Sci. Rep.*, vol. 8, pp. 7571, 2018.

- [49] M. Patel, S. Mishra, R. Verma, and D. Shikha, "Synthesis of ZnO and CuO nanoparticles via Sol gel method and its characterization by using various technique", *Discover Materials*, vol. 2, no. 1, pp. 1, 2022.
- [50] Y. Zare, "Study of Nanoparticles Aggregation/Agglomeration in Polymer Particulate Nanocomposites by Mechanical Properties", *Composites Part A: Applied Science and Manufacturing*, vol. 84, pp. 158-164, 2016.
- [51] I. Khan, K. Saeed, and I. Khan, "Nanoparticles: Properties, Applications and Toxicities", *Arabian Journal of Chemistry*, vol. 12, no. 7, pp. 908-931, 2019.
- [52] A.R. Zanatta, "Revisiting the optical bandgap of semiconductors and the proposal of a unified methodology to its determination, Scientific Report-nature report, vol. 9, pp. 11225, 2019.
- [53] A. Tadj, A. Abderrahmane, M. Zerdali, and S. Hamzaoui, "Facile preparation of nanostructured ZnO via low-temperature hydrothermal method upon changing the precursor anion: The study of structural, morphological, and optical properties", *Materials Today Communications*, vol. 31, pp. 103789, 2022.
- [54] K.P. Misra, S. Jain, A. Agarwala, N. Halder, and S. Chattopadhyay, "Effective Mass Model Supported Band Gap Variation in Cobalt-Doped ZnO Nanoparticles Obtained by Co-precipitation", *Semiconductors*, vol. 54, pp. 3, 2020.
- [55] P. Laokul, N. Kanjana, R. Ratchatane, S. Ruangjan, N. Kotsarn, A. Chingsungnoen, and P. Poolcharuansin, "Preparation of AgBr decorated ZnO/ZnS nanocomposite for photocatalytic and antibacterial applications", *Materials Chemistry and Physics*, vol. 295, pp. 127112, 2023.
- [56] Mohammada, A., Al-Jafa, H. A., Ahmeda, H. S., Mohammedb, M., and Khodairc, Z, Structural and morphological studies of ZnO nanostructures. *Journal of Ovonic Research*, Vol.18, No.3, pp. 443-452, 2022.
- [57] Alwadai, N., Investigation on Structural, Optical, Thermal, and Dielectric Properties of Nanocomposite Films Based on Chitosan Containing Vanadium Pentoxide/Zinc Oxide and Their Potential for Optoelectronics Devices. *Journal of Molecular Structure*, 1312, 138491, 2024.
- [58] Hisham, F., Akmal, M. M., Ahmad, F. B., & Ahmad, K., Facile Extraction of Chitin and Chitosan from Shrimp Shell. *Materials Today: Proceedings*, Vol. 42, pp. 2369-2373, 2021.
- [59] Prasetyaningrum, A., Wicaksono, B. S., Hakiim, A., Ashianti, A. D., Manalu, S. F. C., Rokhati, N., Utomo, D.P., dan Djaeni, M., Ultrasound-Assisted Encapsulation of Citronella Oil in Alginate/Carrageenan Beads: Characterization and Kinetic Models. *ChemEngineering*, 7(1), 10, 2023.
- [60] Arya, S., Mahajan, P., Mahajan, S., Khosla, A., Datt, R., Gupta, V., Young S.J., & Oruganti, S. K., Influence of processing parameters to control morphology and optical properties of Sol-Gel synthesized ZnO nanoparticles. *ECS Journal of Solid State Science and Technology*, 10(2), 023002, 2021.
- [61] Singh, A., Wan, F., Yadav, K., Salvi, A., Thakur, P., & Thakur, A., Synergistic effect of ZnO nanoparticles with Cu²⁺ doping on antibacterial and photocatalytic activity. *Inorganic Chemistry Communications*, 157, 111425, 2023.